Int. J. Electrochem. Sci., 16 **(2021)** 210218, doi: 10.20964/2021.02.16

International Journal of
ELECTROCHEMICAL
SCIENCE
www.electrochemsci.org

Short Communication

Co@N-doped Porous Carbon Derived from Co-MOFs as an Efficient Bifunctional Electrocatalysts for Full Water Splitting

Min Zhao[1,2] *, Changjuan Hu*[1]*, Gaoliang Zhou*[1]*, Xinyi Shen*[1]*, Wei Tan*[1]*, Jianguo Lv*[1,2,*] *, Shengjie Sun*[1]*, Yuxuan Ma*[1]*, Ying Wang*[1]*, Junjun Zhang*[1]*, Jin Yang*[1]*, Miao Zhang*[2,3,*]*, Gang He*[3,*]*, Lei Yang*[4]

[1] School of Physics and Materials Engineering, Hefei Normal University, Hefei 230601, China
[2] Key Laboratory for Photoelectric Detection Science and Technology of Education Department of Anhui Province, Hefei Normal University, Hefei 230601, China
[3] School of Physics and Material Science, Anhui University, Hefei 230039, China
[4] Department of Chemistry and Materials Engineering, Hefei University, Hefei 230601, China
[*]E–mail: lvjg1@163.com (J. Lv), zhmiao@ahu.edu.cn (M. Zhang), hegang@ahu.edu.cn (G. He).

Received: 14 September 2020 / *Accepted:* 22 November 2020 / *Published:* 31 December 2020

Co@N-doped porous carbon were prepared by a one-step pyrolysis method derived from Co-MOFs. The obtained Co@N-doped porous carbon have a large number of metallic Co nanoparticles and contain considerable mesopores. The result indicate that the Co@NC materials exhibit high degree of graphitization. The sample of Co-1.4@NC has the largest grain size of cobalt and high specific surface area of with massive mesopores. As a remarkable bifunctional electrocatalysts, Co-1.4@NC presents remarkable hydrogen evolution reaction (HER) and oxygen evolution reaction (OER) activities in alkaline medium for overall water splitting to produce O_2 and H_2. The result may be attributed to the rich catalytic active species as well as superior electrical conductivity, highsurface area and the porous structure. The cost-effective, highly active and stable Co@NC electrocatalysts have great potential for application in electrocatalytic overall water splitting and fuel cells.

Keyword: Co@N-doped porous carbon; Hifunctional electrocatalysts; Hydrothermal method; oxygen evolution reactions

1. INTRODUCTION

At present, the global environmental and energy problems become more and morn serious. It is extremely urgent to develop environmentally friendly renewable energy, such as wind energy, solar energy and hydrogen energy. Among them, hydrogen energy has been considered as the most promising alternative energy for traditional fossil energy[1-3]. So far, the full water splitting is an effective method to generate hydrogen and oxygen. The electrocatalytic efficiency is closely related to

hydrogen evolution reaction (HER) and oxygen evolution reaction (OER). However, electrochemical full water splitting general needs high-efficient electrocatalysts to overcome the high overpotential and slow kinetic. Noble metals and noble metal-based compounds (such as Pt and RuO_2 catalysts), which exhibit low overpotential and good stability, have been regarded as the most active electrocatalyst for HER and OER. However, high price and low abundance of noble metals limit its large scale commercialization applications. Therefore, noble-metal-free catalysts including transition metal oxides[4], sulfides[5, 6], phosphides [7, 8], selenides[9] and nitrides[10] have been developed for HER and OER in recent years. Moreover, high efficiency electrocatalysts with bifunctional catalytic activities toward HER and OER in the same electrocatalyst play impotant role in full water splitting. In most cases, efficient HER and OER catalytic activity and stability can not be obtained in a same electrocatalyst. Research shows that the electrocatalysts of transition metal (e.g., Fe, Co, Ni) oxide or sulfide active species combined with carbon-based materials(e.g., graphene, carbon nanotubes) exhibits excellent electrocatalytic activities for HER and OER[11-13]. These multifunctional electrocatalysts may apply to fuel cells, zinc-air batteries and electrocatalytic water splitting.

In addition, the efficiency of electrocatalysts can be improved by preparing the micro/nano-architectures with high specific surface area. Different approaches, such as chemical vapor deposition [14], electrodeposition[15], hydrothermal[16], and pyrolysis method[17], have been adopted to synthetize carbon-based nanomaterials with different topographies. Among them, the pyrolysis as a simple and low cost method can be used to prepare N-doped porous carbon with high specific surface area and porosity. However, the mechanism of synthesis and physicochemical properties of the carbon-based electrocatalysts are not clear.

Here, we report the synthesis of Co@N-doped porous carbon by a simple pyrolysis method. The microstructure, specific surface area and porosity of the samples were investigated by means of X-ray diffraction and N_2 adsorption-desorption isotherm. Electrocatalytic test results indicate that the Co@N-doped porous carbon exhibits excellent bifunctional electrocatalytic activities for HER and OER. The electrocatalytic mechanisms have been investigated in detail.

2. EXPERIMENTAL

In a typical procedure, 1, 4-benzenedicarboxylic acid ($C_8H_6O_4$ 0.7g), triethylenediamine ($C_6H_{12}N_2$, 0.22g) and a certain amount of cobalt nitrate hexahydrate ($Co(NO_3)_2{\cdot}6H_2O$, 1.0, 1.4 or 2.2 g) were dispersed in 50 mL of N, N-dimethylformamide (DMF). The mixed solutions were placed in the water bath at the temperature of 60 ℃ and kept stirring for 30 minutes until the solutes completely dissolved. Then the mixed solutions were transferred to a 100 ml autoclave. The autoclave is heated for 24 hours at 120 ℃ in a bake oven. After that, it can be taken out after that the autoclave is cooled to room temperature. Finally, the powders were washed twice with DMF and anhydrous ethanol, respectively. In order to obtain the Co-MOFs, the powders were dried in a vacuum bake oven at 60 ℃ for 24 hours. The obtained Co-MOFs powders were placed in the center of corundum boat, which were placed in a tubular furnace at the temperature of 800℃ for 2 h with a heating rate of 10℃ min^{-1} in N_2 atmosphere. The final powders were named as Co-1.0@NC, Co-1.4@NC and Co-2.2@NC.

The phase of the samples was measured by X-ray diffraction (XRD, TD-3500) Cu K*a* radiation, which operated at 30 kV and 40 mA. Raman spectra of the samples were investigated by a Raman spectroscopy (inVia-Reflex, Renishaw). The surface area and porosity of samples were measured at 77 K using a surface area and porosity analyzer (V-Sorb 4800). Linear sweep voltammetry (LSV) curves from -1.6 to 1 V (vs. Ag/AgCl) were examined with a scan rate of 10 mV s^{-1} at room temperature in 1 M KOH. All potentials were iR-compensated. Before LSV curves test, the products were activated for 20 cycles by using cyclic voltammetry (CV) measurement. Electrochemical impedance spectroscopy (EIS) of the products were evaluated by applying an AC voltage with 5 mV amplitude in a frequency range from 100,000 to 0.01 Hz. All the potentials *versus* Ag/AgCl electrode ($E_{Ag/AgCl}$) were converted into potentials *versus* reversible hydrogen electrode (E_{RHE}) according to the following relation [18]: $E_{RHE} = E_{Ag/AgCl} + 0.059pH + 0.197$. Electrochemical stability was evaluated using current density-time (*I-t*) curve, which was carried out at overpotentials of 207 mV in 1.0 M KOH[19].

3. RESULTS AND DISCUSSION

Figure 1 shows the X-ray diffraction (XRD) patterns of the Co-1.0@NC, Co-1.4@NC and Co-2.2@NC. It can be seen that the three main diffraction peaks in the XRD pattern centered at about 44.21°, 51.52° and 75.85° can be assigned to the (111), (200), and (220) planes of metallic Co (PDF no. 89-4307), respectively[19].

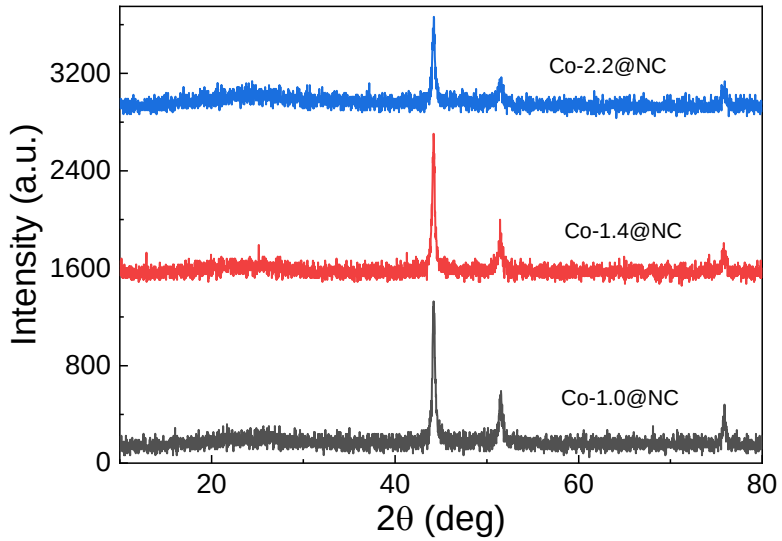

Figure 1. XRD patterns of the samples

In order to estimate the crystallinity of metallic cobalt, the average grain size of cobalt particles could be calculated by Debye-Scherrer formula [20]:

$$D = 0.9\lambda / \beta \cos\theta \qquad (1)$$

where D is the average grain size, λ is the X-ray wavelength (λ= 0.15418 nm), β is the full width at half maximum (FWHM) of the diffraction peak, and θ is the diffraction angle. The average grain size of the thin film has been listed in Table 1. This result indicates the metallic cobalt nanoparticles were successfully embedded in the porous carbon matrix. When the addition amount of cobalt nitrate hexahydrate is 1.4g, the grain size of cobalt reaches the maximum.

Table 1. Average grain size and I_D/I_G of the samples

Sample	D (nm)	I_D/I_G
Co-1.0@NC	19.4	0.90
Co-1.4@NC	24.9	0.98
Co-2.2@NC	22.4	0.98

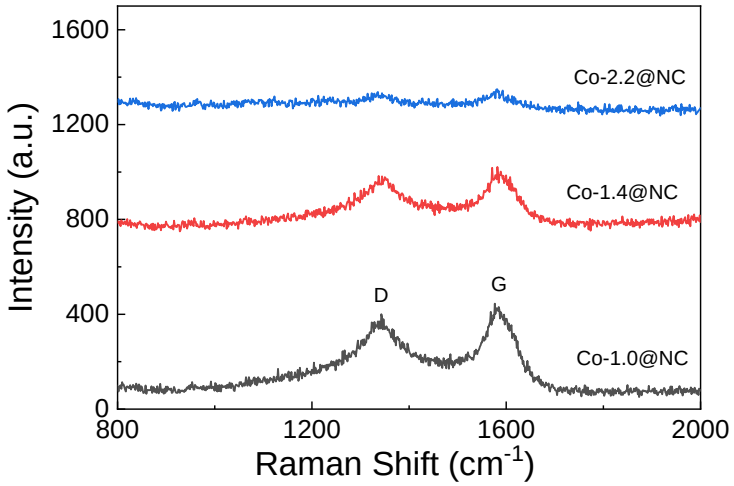

Figure 2. Raman spectra of the samples

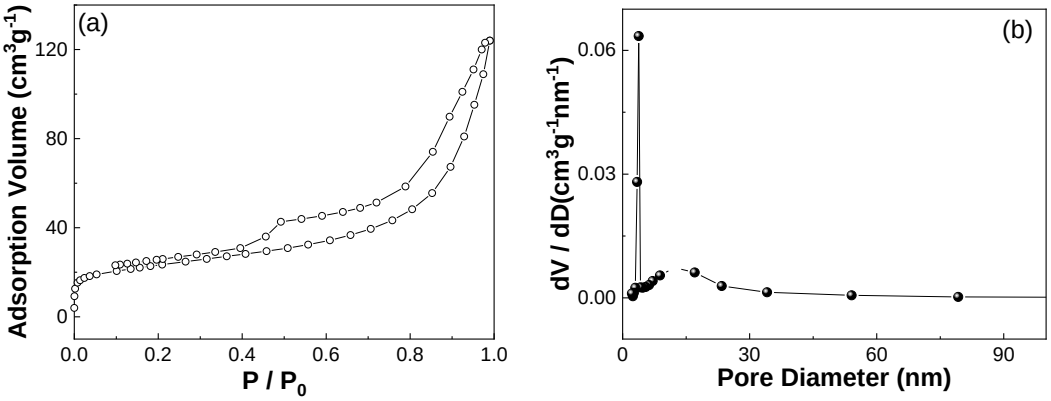

Figure 3. (a)N_2 adsorption-desorption isotherm of the Co-1.4@NC sample. (b) The pore diameter distribution curve.

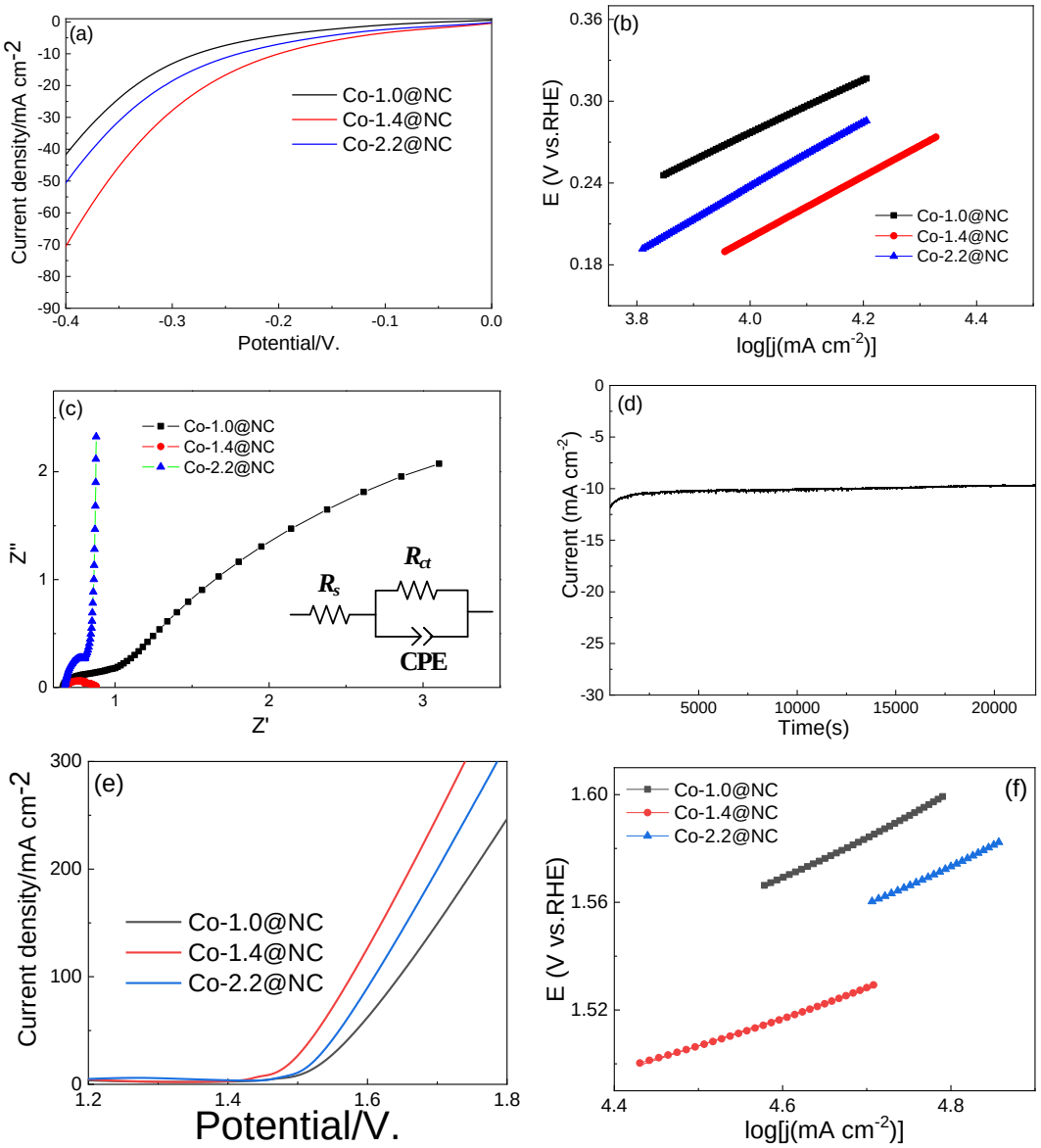

Figure 4. (a) Linear sweep voltammetry curves of Co-1.0@NC, Co-1.4@NC and Co-2.2@NC for HER 0.1 M KOH solution. (b) Tafel plots of Co-1.0@NC, Co-1.4@NC and Co-2.2@NC for HER. (c) Electrochemical impedance spectrum (EIS) of Co-1.0@NC, Co-1.4@NC and Co-2.2@NC recorded in 0.1 M KOH solution and the corresponding equivalent circuit diagram (inset). (d) The current density time (*I*-t) curve of Co-1.4@NC in 1.0 M KOH solution at an overpotential of 230 mV for 6 h. (e) Linear sweep voltammetry curves of Co-1.0@NC, Co-1.4@NC and Co-2.2@NC for OER 0.1 M KOH solution. (f) Tafel plots of Co-1.0@NC, Co-1.4@NC and Co-2.2@NC for OER.

Fig. 2 shows the Raman spectra of the samples. The results show that all of the Raman spectra present the Raman vibration peaks centered at approximate 1343 and 1581 cm^{-1}, which can be assigned to the D-band and G-band of carbon materials. The peak intensity ratio of the *D*-band and *G*-band (I_D/I_G) is associated with the amount of structural defects and disorder in the porous carbon

structures[18]. It can be seen that the I_D/I_G values of the samples are less than 1, which indicate that the degree of graphitization is high in the Co@NC materials[21].

The specific surface area and porosity of the samples were measured by means of N_2 adsorption-desorption isotherm[22]. As shown in Fig. 3a, the Co-1.4@NC presents a type-IV isotherm with an evident hysteresis loop. The result indicate that a mesoporous structure exists in the sample [23]. The surface area of the sample is 81.5m^2 g^{-1}. Fig. 3b presents the BJH pore diameter distribution curve. It also can be seen that the presence of well-defined mesoporosity in the narrow pore diameter rage of 2.8-4.2 nm[22]. High specific surface area of Co-1.4@NC with massive mesopores is beneficial to the exposure of catalytic active sites and rapid transport of HER and OER relevant species.

It is valuable to develop the electrocatalyst with bifunctional OER and HER activities for overall water splitting to produce O_2 and H_2. Fig. 4a shows the polarization curves of all the catalysts for HER. The overpotentials at a current density of 10 mA cm^{-2} are 280, 200 and 240 mV for Co-1.0@NC, Co-1.4@NC and Co-2.2@NC, respectively. It can be seen that the Co-1.4@NC catalyst exhibits the lowest overpotential at the current density of 10 mA cm^{-2} and the best HER catalytic activity. The results indicate that moderate Co doping in the porous carbon structure is important to the HER activity. Fig. 4b presents the Tafel plots of the samples, which calculated from the corresponding polarization curves. The values of the Tafel slopes are 198, 225, and 240 mV dec^{-1} for Co-1.0@NC, Co-1.4@NC and Co-2.2@NC, respectively. The lower value of Tafel slope, indicating the better kinetic process of HER [11]. The stronger the charge transfer ability, the better the electrocatalytic performance. In order to find out the reason of high electrocatalytic activity, EIS of Co-1.0@NC, Co-1.4@NC and Co-2.2@NC was investigated to determine their charge transfer ability. Nyquist plots of the samples have been shown in the Fig. 3c. The charge transfer resistance (R_{ct}), which is associated with the electrocatalytic kinetics in catalyst/electrolyte interface, can be calculated by means of fitting Nyquist plots with an equivalent circuit model [2]. The values of R_{ct} are 0.810, 0.228 and 0.989Ω for Co-1.0@NC, Co-1.4@NC and Co-2.2@NC, respectively. The result indicates that the Co-1.4@NC has the smallest charge transfer resistance (R_{ct}). Therefore, the stronger charge transfer capacity and the larger specific surface area with porous morphology is responsible for the high electrocatalytic activity of Co-1.4@NC for HER. The long-term durability of the Co-1.4@NC for the HER was surveyed at an overpotential of 230 mV for 6h. It can be seen from the Fig. 4d that the cathodic current density is almost not changed over 12 h. The outstanding stability may be attributed to the moderate amount of cobalt doping and stable structure of Co-1.4@NC. In order to investigate the bifunctional activities in the same electrolyte, the electrocatalytic OER performance of the samples also have been measured in 1 M KOH. Fig.4e shows the corresponding polarization curves, which have been ed from linear sweep voltammetry (LSV) measurements. The overpotentials at a current density of 10 mA cm^{-2} are 270, 230 and 260 mV, respectively. Tafel plots (Fig. 4f) were calculated according to the corresponding polarization curves. The values of the Tafel slopes are 155, 104 and 146 mV dec^{-1} for Co-1.0@NC, Co-1.4@NC and Co-2.2@NC, respectively. It can be seen that the Co-1.4@NC has the lowest overpotential value and the minimum Tafel slope among all the samples, indicating it has the high OER activity. It is believed that the high OER activity may be attributed to the rich catalytic

active species as well as superior electrical conductivity, high surface area and the porous structure [11].

4. CONCLUSION

In summary, Co@N-doped porous carbon have been successfully prepared from Co-MOFs by a facile pyrolysis method. It has been found that content of cobalt nitrate hexahydrate has important effect on the microstructure and electrocatalytic hydrogen evolution reaction (HER) and oxygen evolution reaction (OER) activities of the samples. The experimental results show that the Co-1.4@NC possesses the highest specific surface area of 81.5 m^2 g^{-1} and massive mesopores with large pore volume of 0.191 cm^3 g^{-1}. The Co-1.4@NC demonstrates preferable bifunctional electrocatalytic activities for HER and OER in alkaline medium. The overpotentials of HER and OER are 200 and 230 mV at current densities of 10 mA cm^{-2}, respectively. The Tafel slope corresponds to polarization curves of HER and OER are 225 and 104 mV dec^{-1}. The strategy presented here may be helpful to develop high performance bifunctional electrocatalysts using Co-MOFs as precursors for electrocatalytic overall water splitting and fuel cells.

ACKNOWLEDGEMENTS
This work was supported by National Natural Science Foundation of China (Nos. 51701001, 61804039, 51802145), Academic funding projects for Top Talents in Subjects (Majors) of Universities (No. gxbjZD31), Natural Science Foundation of Anhui Higher Education Institution of China (KJ2019A0734, KJ2017A924, KJ2017A002, KJ2019A0735), Natural Science Foundation of Anhui Province (No. 1808085QE126) and Universities Joint Key Laboratory of Photoelectric Detection Science and Technology in Anhui Province(Grant No. 2020GDTCZD01).

References

1. J. Hu, J. Chen, H. Lin, R. Liu and X. Yang, *J. Solid State Chem.*, 259 (2018) 1.
2. W.H. Guo, Q. Zhang, X.H. Wang, Y.X. Yang, X.L. Li, L.J. Li, H.Q. Luo and N.B. Li, *Electrochim. Acta*, 357 (2020) 136850.
3. Y. Wang, Y. Pan, L. Zhu, H. Yu, B. Duan, R. Wang, Z. Zhang and S. Qiu, *Carbon*, 146 (2019) 671.
4. G. Mohan Kumar, P. Ilanchezhiyan, C. Siva, A. Madhankumar, T.W. Kang and D.Y. Kim, *Int. J. Hydrogen Energy*, 45 (2020) 391.
5. J. Ding, S. Ji, H. Wang, H. Gai, F. Liu, V. Linkov and R. Wang, *Int. J. Hydrogen Energy*, 44 (2019) 2832.
6. Y. Zhou, M. Luo, Z. Zhang, W. Li, X. Shen, W. Xia, M. Zhou and X. Zeng, *Appl. Surf. Sci.*, 448 (2018) 9.
7. L. Peng, S.S.A. Shah and Z. Wei, *Chinese J. Catal.*, 39 (2018) 1575.
8. Y. Wang, B. Kong, D. Zhao, H. Wang and C. Selomulya, *Nano Today*, 15 (2017) 26.
9. X. Peng, Y. Yan, X. Jin, C. Huang, W. Jin, B. Gao and P.K. Chu, *Nano Energy*, 78 (2020) 105234.
10. K.C. Majhi and M. Yadav, J. Alloys Compd., 855 (2021) 157511.
11. X. Zhang, S. Liu, Y. Zang, R. Liu, G. Liu, G. Wang, Y. Zhang, H. Zhang and H. Zhao, *Nano Energy*, 30 (2016) 93.

12. X. Guo, W. Zhang, D. Zhang, S. Qian, X. Tong, D. Zhou, J. Zhang and A. Yuan, *ChemElectroChem*, 6 (2019) 4571.
13. Y. Peng and S. Chen, *Green Energy Environ.*, 3 (2018) 335.
14. Z. Ali, M. Mehmood, J. Ahmed and M.N. Nizam, *Nano-Structures & Nano-Objects*, 24 (2020) 100574.
15. X. Zhang, X. Shi and C. Wang, *Catal. Commun.*, 10 (2009) 610.
16. T. Zhou, R. Ma, Y. Zhou, R. Xing, Q. Liu, Y. Zhu and J. Wang, *Microporous Mesoporous Mater.*, 261 (2018) 88.
17. S. Li, Q. Zhou, G. Yu, Z. Lei, Z. Liu, Q. Xu, W. Xu and R. Wu, *Appl. Surf. Sci.*, 518 (2020) 146239.
18. R. Liu, H. Zhang, X. Zhang, T. Wu, H. Zhao and G. Wang, *RSC Adv.*, 7 (2017) 19181.
19. H. Li, X. Qian, C. Xu, S. Huang, C. Zhu, X. Jiang, L. Shao and L. Hou, *ACS Appl. Mater. Interfaces*, 9 (2017) 28394.
20. J. Lv, W. Wang, M. Zhao, Y. Cheng, W. Zhu, G. He, M. Zhang, Z. Sun and X. Chen, *J. Mater. Sci. Mater. Electron.*, 28 (2017) 1022.
21. S. Wang, G. Zhou, J. Lv, Y. Ma, Y. Wang, C. Hu, J. Zhang, J. Yang, G. He, M. Zhang, M. Zhao, X. Chen and L. Yang, *J. Phys. Chem. Solids*, 148 (2021) 109696.
22. S. Peng, L. Li, S.G. Mhaisalkar, M. Srinivasan, S. Ramakrishna and Q. Yan, *ChemSusChem*, 7 (2014) 2212.
23. F. Bai, H. Huang, C. Hou and P. Zhang, *New J. Chem.*, 40 (2016) 1679.